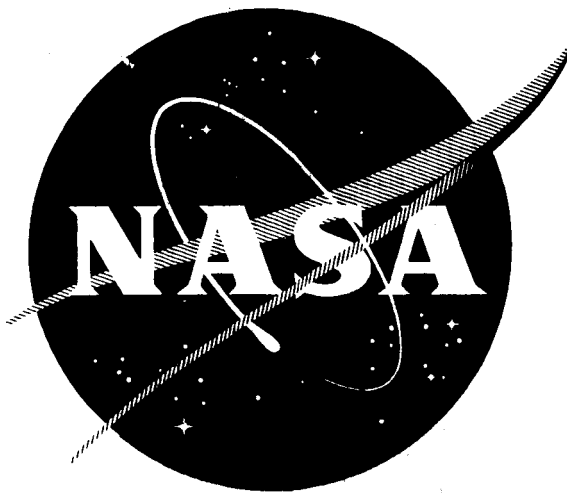


*N.I.*

WANL-PR-(Q)-014  
NASA-CR-72306



# DEVELOPMENT OF DISPERSION STRENGTHENED TANTALUM BASE ALLOY

Thirteenth Quarterly Report

by

R. W. Buckman and R. C. Goodspeed

prepared for

National Aeronautics and Space Administration

Lewis Research Center

Space Power Systems Division

Under Contract (NAS 3-2542)



## ASTRONUCLEAR LABORATORY

## WESTINGHOUSE ELECTRIC CORPORATION

N68-13630

(ACCESSION NUMBER)

(THRU)

(PAGES)

(CODE)

(NASA CR OR TMX OR AD NUMBER)

(CATEGORY)

FACILITY FORM 602

GPO PRICE \$

CFSTI PRICE(S) \$

Hard copy (HC) \$3.00

Microfiche (MF) .65

ff 653 July 65

## NOTICE

This report was prepared as an account of Government-sponsored work. Neither the United States nor the National Aeronautics and Space Administration (NASA), nor any person acting on behalf of NASA:

- A) Makes any warranty or representation, expressed or implied, with respect to the accuracy, completeness, or usefulness of the information contained in this report, or that the use of any information, apparatus, method, or process disclosed in this report may not infringe privately-owned rights; or
- B) Assumes any liabilities with respect to the use of, or for damages resulting from the use of any information, apparatus, method or process disclosed in this report.

As used above, "person acting on behalf of NASA" includes any employee or contractor of NASA, or employee of such contractor, to the extent that such employee or contractor of NASA or employee of such contractor prepares, disseminates, or provides access to, any information pursuant to his employment or contract with NASA, or his employment with such contractor.

Copies of this report can be obtained from:

National Aeronautics & Space Administration  
Office of Scientific and Technical Information  
Washington 25, D. C.  
Attention: AFSS-A

001127

DEVELOPMENT OF DISPERSION STRENGTHENED  
TANTALUM BASE ALLOY

by

R. W. Buckman, Jr.

and

R. C. Goodspeed

THIRTEENTH QUARTERLY PROGRESS REPORT

Covering the Period

November 20, 1966 - February 20, 1967

Prepared For

NATIONAL AERONAUTICS AND SPACE ADMINISTRATION  
Contract NAS 3-2542

Technical Management  
Paul E. Moorhead  
NASA-Lewis Research Center  
Space Power Systems Division

Astronuclear Laboratory  
Westinghouse Electric Corporation  
Pittsburgh 36, Pa.

PRECEDING PAGE BLANK NOT FILMED.

## ABSTRACT

Development of dispersion strengthened tantalum base alloys for use in advanced space power systems continued as the evaluation of Ta-8W-1Re-1Hf (ASTAR-811) and Ta-7W-1Re-1Hf-0.012C-0.012N (ASTAR-811CN) sheet material was essentially completed. Tensile properties of TIG welded sheet specimens of both alloys were determined over the temperature range of  $-320$  to  $2600^{\circ}\text{F}$ . One hour post weld anneals at temperatures ranging from  $1800$  to  $2600^{\circ}\text{F}$  resulted in an increase in the ductile-brittle transition temperature of TIG welded ASTAR-811CN, while the transition temperature of TIG welded ASTAR-811 remained below  $-320^{\circ}\text{F}$ . Phase identification studies on ASTAR-811CN indicated that the HCP tantalum dimetal carbide is the precipitate which occurs during processing to 0.04 inch sheet and short time anneals. The FCC carbonitride phase occurs at the expense of the dimetal carbide during longer ( $\geq 16$  hours) anneals at temperatures of about  $2400^{\circ}\text{F}$  and higher. The scope of work this period was expanded to include an investigation of the effect of grain size and annealing temperatures on the creep properties of ASTAR-811, ASTAR-811CN, and ASTAR-811C (Ta-8W-1Re-0.7Hf-0.025C). Grain size data were obtained on these alloys as a function of annealing time and temperature.

## TABLE OF CONTENTS

|  | <u>Page No.</u> |
|--|-----------------|
| I. INTRODUCTION  | 1               |
| II. PROGRAM STATUS   | 2               |
| A. EFFECT OF THERMAL TREATMENT ON CREEP BEHAVIOR               | 2               |
| B. INTERSTITIAL ELEMENT LOSSES DURING VACUUM<br>HEAT TREATMENT | 7               |
| C. WELDABILITY   | 11              |
| D. MECHANICAL PROPERTIES                                       | 20              |
| III. FUTURE WORK   | 29              |
| IV. REFERENCES   | 31              |

## LIST OF FIGURES

|  | <u>Page No.</u> |
|--|-----------------|
| 1. Grain Size of ASTAR-811, ASTAR-811C, and ASTAR-811CN as a Function of Annealing Time and Temperature                              | 5               |
| 2. Parabolic Rate Constant for Grain Growth of ASTAR-811, ASTAR-811C, and ASTAR-811CN as a Function of Reciprocal Temperature        | 6               |
| 3. Carbon and Nitrogen Losses in Unwrapped and Wrapped ASTAR-811CN as a Function of Time at 2100°C                                   | 9               |
| 4. Total Interstitial Losses in Unwrapped and Wrapped ASTAR-811CN as a Function of Time at 2100°C                                    | 10              |
| 5. Ductile-Brittle Transition Temperature Test Results for Post (TIG) Weld Annealed ASTAR-811CN                                      | 13              |
| 6. Results of Hardness Traverses Across As-Welded Specimens of ASTAR-811 and ASTAR-811CN   | 15              |
| 7. Representative Microstructures of TIG Welded ASTAR-811  | 16              |
| 8. Microstructure of Weld Zone/Heat Affected Zone Interface in TIG Welded ASTAR-811C Specimen After 1 Hr. Post Weld Anneal at 1200°C | 17              |
| 9. Microstructures of TIG Welded ASTAR-811CN Specimens After 1 Hr. Post Weld Anneals at Various Temperatures                         | 18              |
| 10. Creep Properties of ASTAR Tantalum Alloys  | 25              |
| 11. Aging Behavior of ASTAR-811CN  | 30              |

## LIST OF TABLES

|  | <u>Page No.</u> |
|--|-----------------|
| 1. Effect of Annealing Temperature and Annealing Time on the Grain Size of ASTAR-811, ASTAR-811C and ASTAR-811CN   | 3               |
| 2. Chemical Analyses of Unwrapped and Wrapped ASTAR-811CN as a Function of Time at 2100°C (3810°F)   | 8               |
| 3. Ductile-Brittle Transition Temperature of Post (TIG) Weld Annealed NASV-23  | 12              |
| 4A. Tensile Properties of TIG Welded ASTAR-811, ASTAR-811C and ASTAR-811CN   | 21              |
| 4B. Tensile Properties of TIG Welded ASTAR-811 and ASTAR-811CN   | 22              |
| 5. Creep Properties of ASTAR-811 and ASTAR-811CN   | 24              |
| 6. X-ray Diffraction Analyses of Various ASTAR-811CN Bulk Extracted Residues   | 27              |
| 7. X-ray Diffraction Analyses of Phases Extracted from ASTAR-811CN Specimens Annealed for 1 Hr. at 1650°C and Aged for 1 and 16 Hrs. at 1090, 1200, 1315, and 1425°C | 28              |

## I. INTRODUCTION

This, the thirteenth quarterly progress report on the NASA-sponsored program, "Development of Dispersion Strengthened Tantalum Base Alloys" describes the work accomplished during the period November 20, 1966 to February 20, 1967. The work was performed under Contract NAS 3-2542.

The primary objective of the current phase of this program is the processing and evaluation of 0.04 inch sheet of three compositions which were melted as 60-pound, 4-inch diameter ingots. The compositions were selected for potential sheet and tubing applications on the basis of weldability, creep resistance, and fabricating characteristics.

Prior to this quarterly period, several promising tantalum alloy compositions were developed which exhibited a good combination of creep resistance, weldability, and fabricability. <sup>(1)</sup> The three compositions selected for scale up are:

|             |                             |
|-------------|-----------------------------|
| ASTAR-811   | Ta-8W-1Re-1Hf               |
| ASTAR-811C  | Ta-8W-1Re-1Hf-0.025C        |
| ASTAR-811CN | Ta-7W-1Re-1Hf-0.012C-0.012N |

These compositions were consumable electrode double vacuum arc melted as 60-pound, 4-inch diameter ingots, which were subsequently processed to 0.04-inch sheet by a combination of forging and rolling. Evaluation of composition Ta-8W-1Re-1Hf-0.025C (ASTAR-811C) has been essentially completed, <sup>(2)</sup> and evaluation of the remaining two compositions Ta-8W-1Re-1Hf (ASTAR-811) and Ta-7W-1Re-1Hf-0.012C-0.012N (ASTAR-811CN), initiated. <sup>(3)</sup>

During this quarterly period the evaluation of weldability, tensile properties, and creep resistance of the Ta-8W-1Re-1Hf (ASTAR-811) and Ta-7W-1Re-1Hf-0.012C-0.012N (ASTAR-811CN) was essentially completed. The scope of the contract was also expanded to include an investigation of the effect of grain size on the creep properties of all three scale-up alloys. To date grain size data has been obtained as a function of annealing time and temperature.



## II. PROGRAM STATUS

### A. EFFECT OF THERMAL TREATMENT ON CREEP BEHAVIOR

The scope of work was changed to include a limited investigation on the effect of final annealing treatment on the creep behavior of the ASTAR-811, ASTAR-811C, and ASTAR-811CN compositions. Prior work<sup>(4)</sup> on ASTAR-811C (Ta-8W-1Re-1Hf-0.025C) has shown that creep behavior is strongly influenced by the final annealing temperature. Increasing the final annealing temperature from 1650°C to 2000°C resulted in a 50% reduction in creep rate. However, the average grain diameter increased from 0.03 mm to 0.18 mm as the 1 hour annealing temperature was increased from 1650°C to 2000°C. In addition there was also a significant change in the precipitate morphology as the annealing temperature was increased.<sup>(4)</sup> Thus it is important to identify the factors contributing to the observed improvement in creep behavior. A series of specimens will be annealed over the temperature range of 1800-2100°C for a time sufficient to produce a final grain size of 0.03 mm, the resulting grain size achieved after the standard final annealing treatment, i. e., 1 hour at 1650°C. The specimens will then be creep tested at 2400°F under an applied stress of 15,000 psi.

During this period, 0.04-inch thick sheet specimens of all three ASTAR compositions were annealed at 1800, 1900, 2000, and 2100°C (3270, 3450, 3630, and 3810°F) for 30, 300, and 900 seconds. The 0.04-inch sheet from which the specimens were taken had been reduced 85% by cold rolling. The average grain diameter determined by the line intercept method and room temperature hardness data are recorded in Table 1. The annealing sequence consisted of slowly heating the furnace to 1200°C while maintaining the chamber pressure at  $\leq 1 \times 10^{-5}$  torr and then heating to the desired temperature as rapidly as possible. Time at temperature was recorded from when the specimen reached a temperature within 50°C of the test temperature. After the specified time at temperature the furnace was shut off and the chamber was back-filled with helium gas to accelerate cooling of the specimens. All specimens were heat treated bare. From these results the heat treatments selected to produce a grain size of 0.03 mm are

TABLE 1 - Effect of Annealing Temperature and Annealing Time on the Grain Size of ASTAR-811, ASTAR-811C, and ASTAR-811CN

| Composition                                  | Annealing Time (min.) | Grain Size (in mm) and Hardness <sup>(1)</sup> for Temperatures, °C/°F |     |       |     |       |     |       |     |       |     |       |     |
|--|-----------------------|--|-----|-------|-----|-------|-----|-------|-----|-------|-----|-------|-----|
|  |                       | 1800   |     | 1900  |     | 2000  |     | 2100  |     | 2000  |     | 2100  |     |
|  |                       | GS   | DPH | GS    | DPH | GS    | DPH | GS    | DPH | GS    | DPH | GS    | DPH |
| ASTAR-811<br>(Ta-8W-1Re-1Hf)                 | 1/2                   | 0.016  | 196 | 0.024 | 199 | 0.029 | 202 | 0.042 | 199 | 0.029 | 202 | 0.042 | 199 |
|  | 5                     | 0.024  | 200 | 0.038 | 196 | 0.077 | 197 | 0.098 | 195 | 0.077 | 197 | 0.098 | 195 |
|  | 15                    | 0.045  | 181 | 0.079 | 194 | 0.118 | 182 | 0.186 | 197 | 0.118 | 182 | 0.186 | 197 |
| ASTAR-811C<br>(Ta-8W-1Re-0.7Hf-0.025C)       | 1/2                   | 0.016  | 263 | 0.021 | 262 | 0.033 | 270 | 0.038 | 254 | 0.033 | 270 | 0.038 | 254 |
|  | 5                     | 0.026  | 267 | 0.030 | 258 | 0.067 | 268 | 0.093 | 256 | 0.067 | 268 | 0.093 | 256 |
|  | 15                    | 0.045  | 271 | 0.065 | 251 | 0.100 | 281 | 0.178 | 255 | 0.100 | 281 | 0.178 | 255 |
| ASTAR-811CN<br>(Ta-7W-1Re-1Hf-0.012C-0.012N) | 1/2                   | 0.013  | 287 | --    | --  | 0.031 | 305 | --    | --  | 0.031 | 305 | --    | --  |
|  | 5                     | 0.026  | 294 | --    | --  | 0.067 | 288 | --    | --  | 0.067 | 288 | --    | --  |
|  | 15                    | 0.039  | 297 | --    | --  | 0.107 | 272 | --    | --  | 0.107 | 272 | --    | --  |

(1) DPH, 30 Kg load.

as follows:

10 minutes at 1800°C/3270°F

5 minutes at 1900°C/3450°F

30 seconds at 2000°C/3630°F

It has been shown that under isothermal conditions, the grain size (D) varies with time (t) according to the following expression:

$$D^2 = K \gamma V t$$

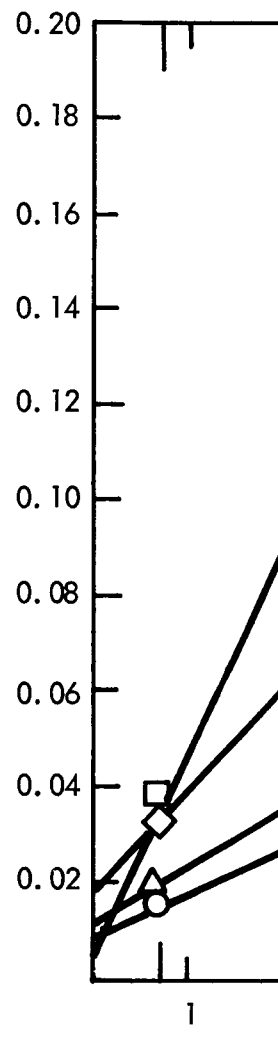
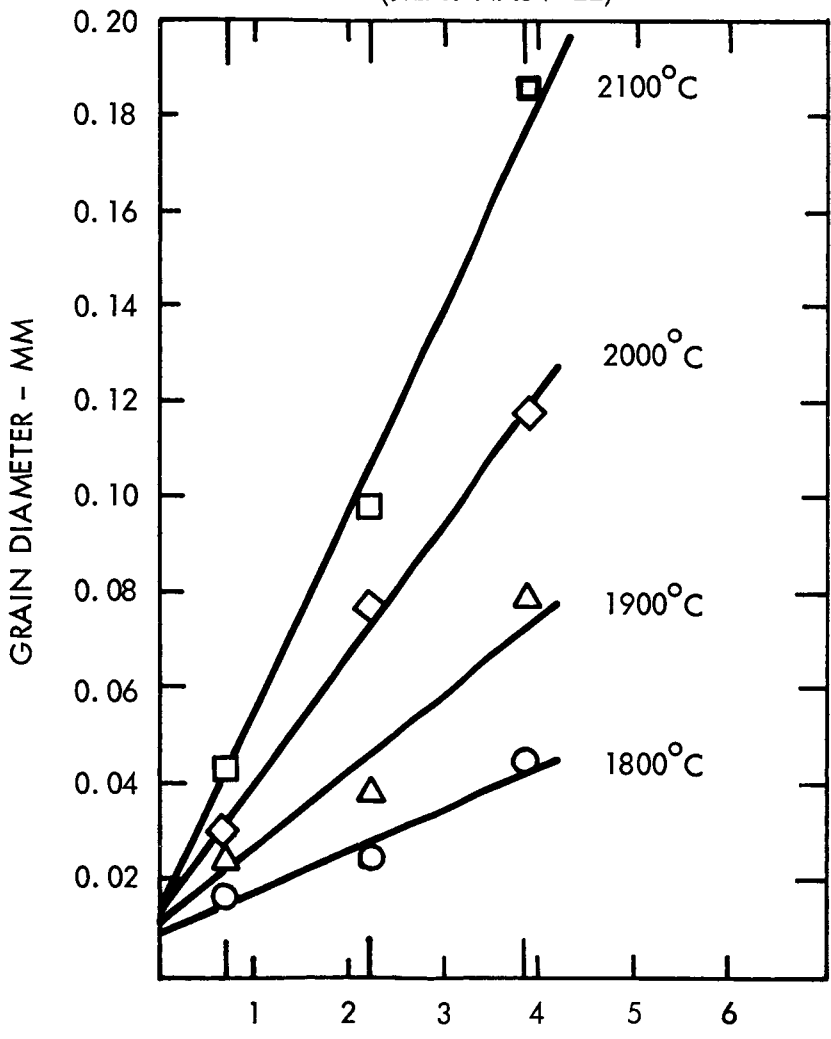
where the surface energy of the boundary ( $\gamma$ ) is the driving force for boundary migration. K is a rate constant and V is the grain atomic volume. Thus at a given temperature, the grain size is proportional to the square root of time. The grain size data in Table 1 when plotted as a function of time (see Figure 1) result in a good linear fit. The slope of this curve  $\frac{\partial D}{\partial t}^{1/2}$  is equal to  $\sqrt{K}$ , the parabolic rate constant which varies with temperature according to the familiar Arrhenius rate equation;

$$K = K_0 \exp^{-Q/RT}$$

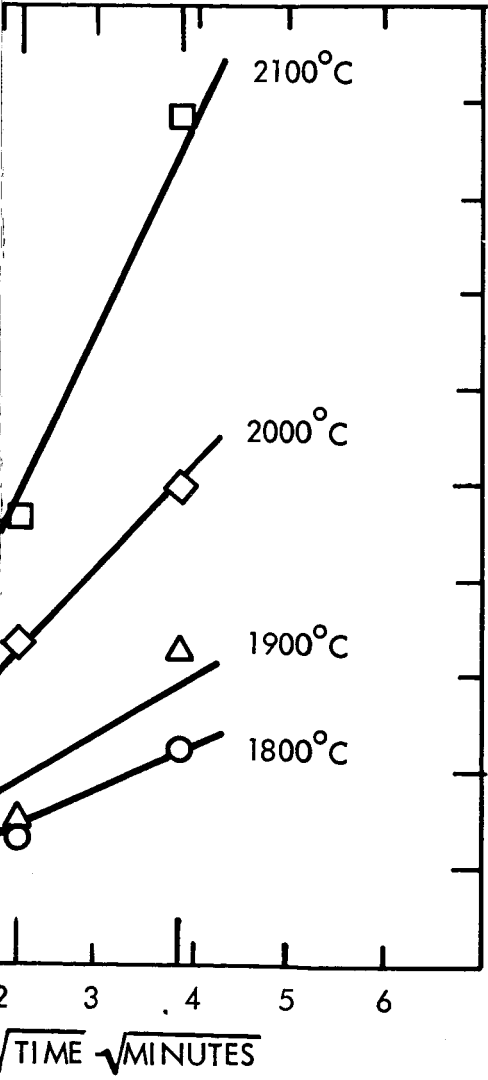
where Q is the activation energy, T is absolute temperature, R is the gas constant, and  $K_0$  a proportionality constant. Thus the activation energy for grain growth can be calculated from the slope of the curve  $D^2/t$  vs  $1/T$ . From the  $D^2/t$  vs  $1/T$  plot in Figure 2, a value of Q of 92 kcal/mole was determined. The activation energy for the self diffusion of tantalum is reported to be 110 kcal/mole<sup>(5)</sup> and it would be expected that the activation energy for grain boundary migration would be less than one-half this value. Thus the value of 92 kcal/mole determined for these tantalum alloys appears to be higher than would normally be expected. The explanation for this apparent high value is not evident.

The grain growth behavior of all three tantalum compositions was identical over the range of test temperatures studied. This would be expected for the ASTAR-811 and ASTAR-811CN since at 1800°C, the solvus for the 0.012C and 0.012N has been exceeded. However, the carbon solvus for the ASTAR-811C which contains 0.025% is not exceeded until heating

ASTAR-811  
(Ta-8W-1 Re-1 Hf)  
(HEAT NASV-22)



ASTAR-811C  
8W-1Re-0.7Hf-0.025C)  
(HEAT NASV-20)



ASTAR-811CN  
(Ta-7W-1Re-1Hf-0.012C-0.012N)  
(HEAT NASV-23)

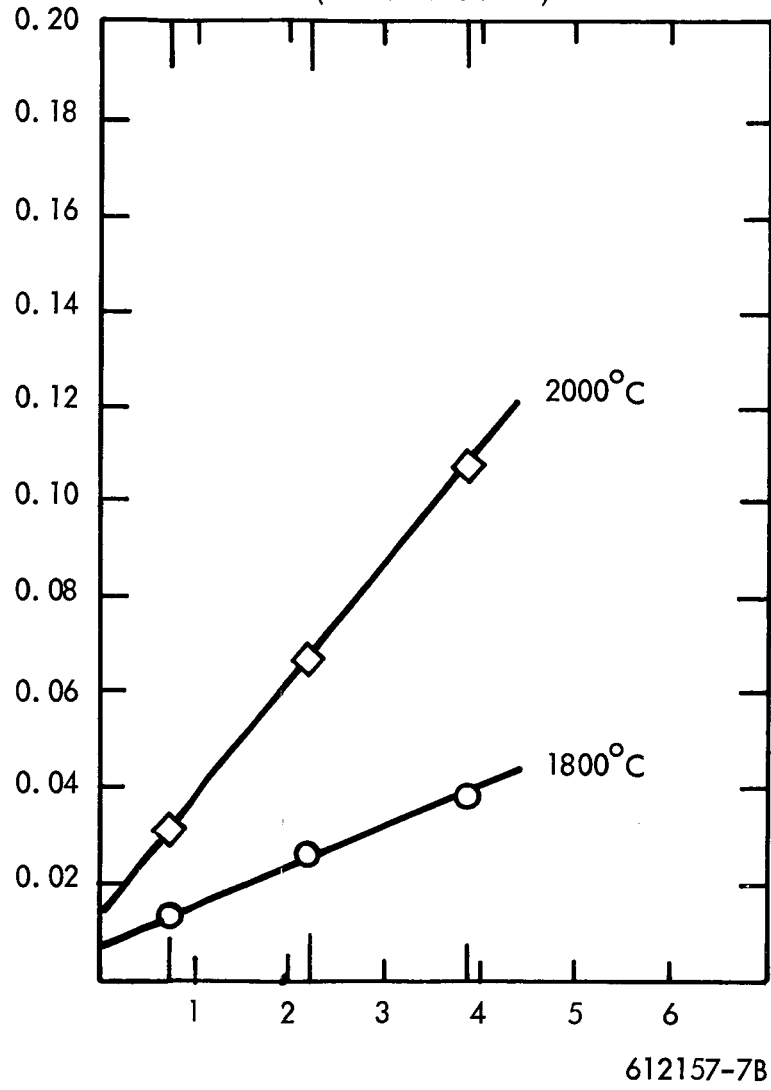


FIGURE 1 - Grain Size of ASTAR-811, ASTAR-811C, and ASTAR-811CN as a Function of Annealing Time and Temperature

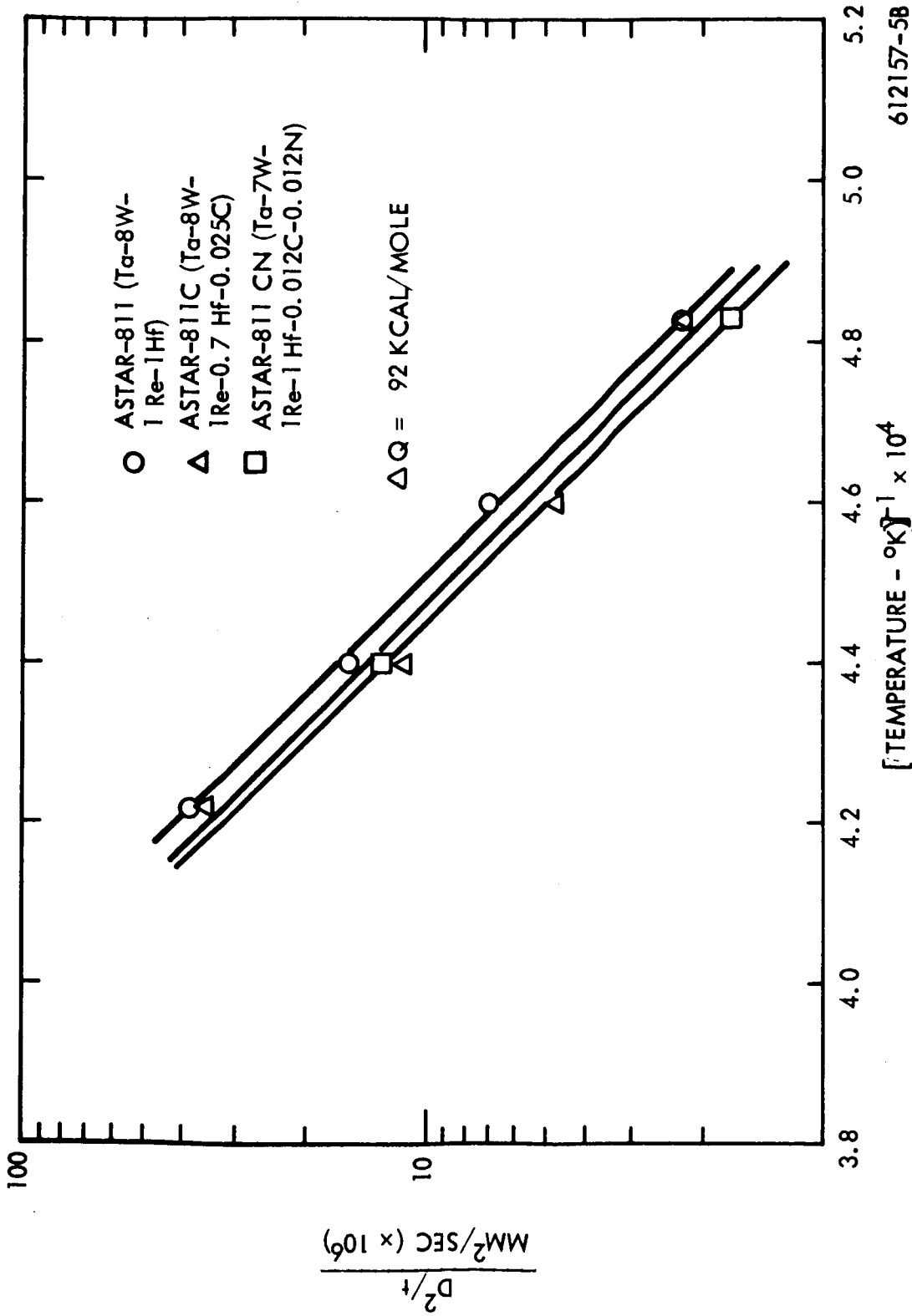


FIGURE 2 - Parabolic Rate Constant for Grain Growth of ASTAR-811, ASTAR-811C, and ASTAR-811CN as a Function of Reciprocal Temperature

above 1900°C. Thus it can be concluded that the carbide particles present at 1800°C do not inhibit grain boundary migration.

## B. INTERSTITIAL ELEMENT LOSSES DURING VACUUM HEAT TREATMENT

The carbide and nitride phases in the tantalum alloy matrix have appeared stable for long time periods over the temperature range of 1800-2600°F when exposed at pressures of  $\leq 1 \times 10^{-8}$  torr. <sup>(6)</sup> However, as discussed previously, the optimum creep characteristics are achieved by using final annealing treatments in the 3200-3600°F temperature range. Current industry wide practice for high temperature vacuum heat treatment is to use unbaked, polymer sealed systems operating at  $10^{-5} - 10^{-4}$  torr. Most heat treatment specifications also require Ta, Cb, or Cb-1Zr foil wrapping of the work piece as a barrier to contamination during the annealing cycle. Decarburization of a carbon containing tantalum alloy at  $1 \times 10^{-5}$  torr at >2000°C was reported early in this investigation. <sup>(7)</sup> It is assumed that the decarburization is via the methane and/or CO reactions similar to that reported for decarburization of molybdenum alloys. It was also shown that wrapping the sample with pure tantalum foil resulted in a greater carbon loss. It is assumed that the foil acts as a sink and that the rate of carbon transfer across the foil interface is faster than the carbon loss due to reaction with the residual H<sub>2</sub>, H<sub>2</sub>O present in the vacuum chamber atmosphere at  $1 \times 10^{-5}$  torr.

Additional vacuum annealing tests were made during the report period on the carbonitride strengthened composition ASTAR-811CN (Ta-7W-1Re-1Hf-0.012C-0.012N). Sheet specimens, 0.04-inch thick, bare and wrapped with tantalum foil, were exposed for 5, 30, and 60 minutes at 2100°C (3810°F). After heat treatment, the samples were then analyzed for carbon and nitrogen content. The analytical results are recorded in Table 2 and graphically illustrated in Figures 3 and 4. Significant carbon and nitrogen losses have occurred during this annealing treatment and confirm the losses observed previously when annealing this composition at 2000°C and above. <sup>(3)</sup> The use of a foil wrapping, while reducing the possibility of oxygen contamination, acts as a sink for carbon. The nitrogen loss is assumed to be by degassing and the foil wrapping appears to retard the rate at which it occurs.

TABLE 2 - Chemical Analyses of Unwrapped and Wrapped<sup>(a)</sup> ASTAR-811CN  
(Ta-7W-1Re-1Hf-0.012C-0.012N) as a Function of Time at  
2100°C/3810°F and  $1 \times 10^{-5}$  Torr in Oil Diffusion Pumped Vacuum System

| Condition <sup>(b)</sup> | Time<br>(min.) | Carbon<br>Content<br>(ppm) | % Carbon<br>Lost | Nitrogen<br>Content<br>(ppm) | % Nitrogen<br>Lost | Total<br>Interstitials<br>Lost |      |
|--------------------------|----------------|----------------------------|------------------|------------------------------|--------------------|--------------------------------|------|
|                          |                |                            |                  |                              |                    | ppm                            | (%)  |
| Unwrapped                | 5              | 96                         | 20               | 64                           | 47                 | 80                             | 33.5 |
|                          | 30             | 64                         | 47               | 49                           | 59                 | 127                            | 53   |
|                          | 60             | 55                         | 54               | 31                           | 74                 | 154                            | 64   |
| Wrapped <sup>(a)</sup>   | 5              | 72                         | 40               | 113                          | 6                  | 55                             | 23   |
|                          | 30             | 82                         | 32               | 70                           | 42                 | 88                             | 37   |
|                          | 60             | 47                         | 61               | 64                           | 47                 | 129                            | 54   |

(a) Specimens wrapped tightly in pure tantalum foil.

(b) Initial carbon and nitrogen content 120 ppm.



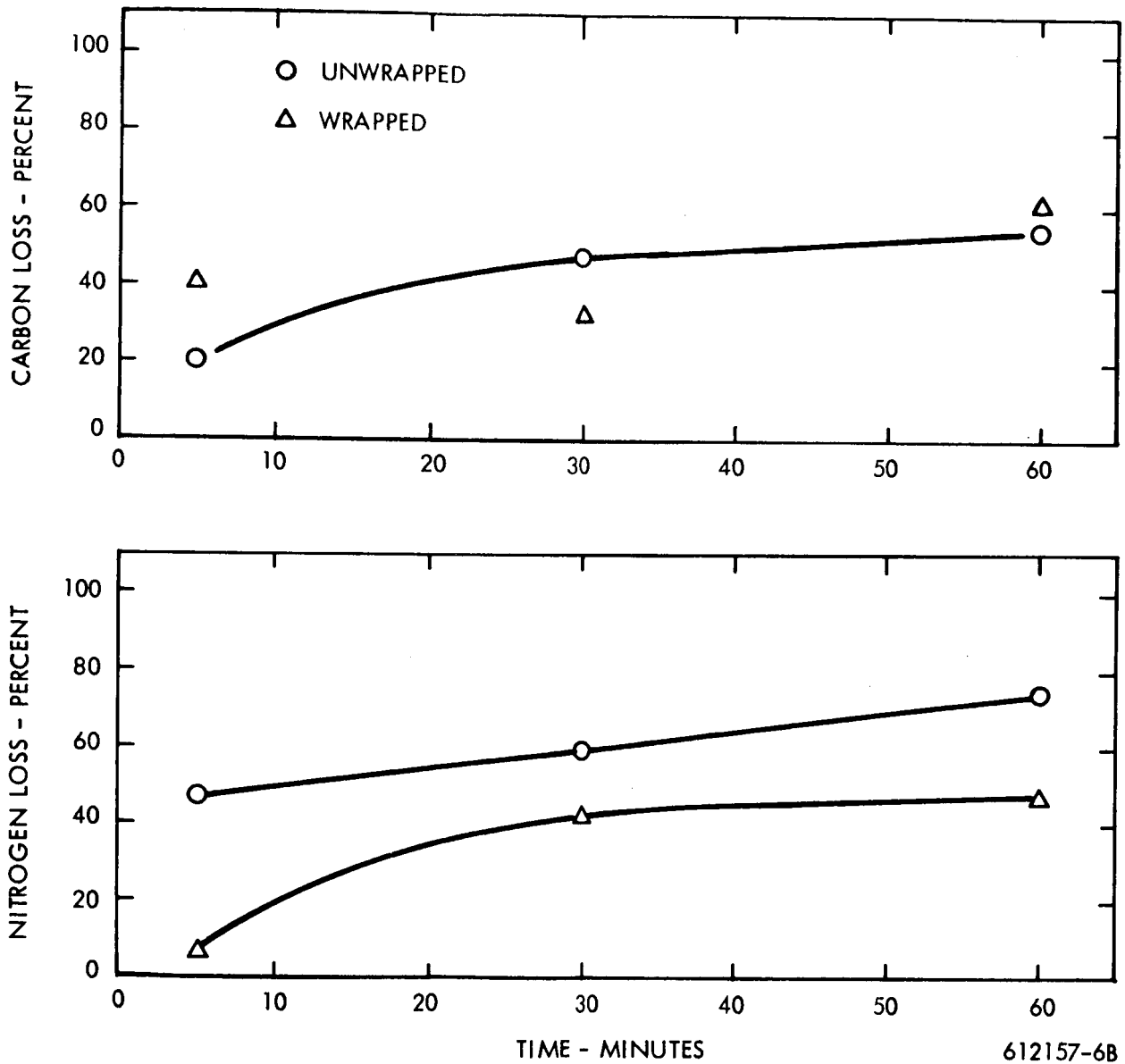


FIGURE 3 - Carbon and Nitrogen Losses in Unwrapped and Wrapped ASTAR-811CN (Ta-7W-1Re-1Hf-0.012C-0.012N) as a Function of Time at 2100°C/3810°F and  $1 \times 10^{-5}$  Torr in Oil Diffusion Pumped System

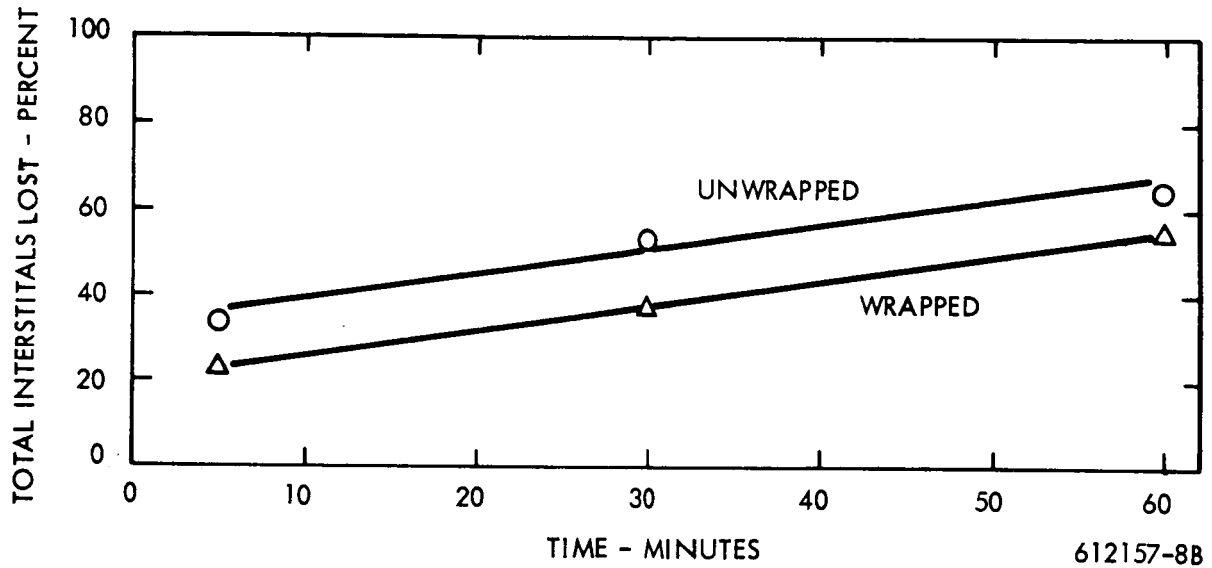


FIGURE 4 - Total Interstitial Losses in Unwrapped and Wrapped ASTAR-811CN (Ta-7W-1Re-1Hf-0.012C-0.012N) as a Function of Time at 2100°C/3810°F and  $1 \times 10^{-5}$  Torr in Oil Diffusion Pumped System

These tests are very preliminary in nature and more detailed work is beyond the scope of this program. But certain obvious implications arise if refractory metal alloys strengthened with carbide and/or nitride dispersions are to be utilized to the fullest. High temperature vacuum annealing treatments on alloys of the type which have been developed during this investigation may have to be accomplished in bakeable ultra-high vacuum systems to prevent carbon loss and with a controlled nitrogen partial pressure to prevent nitrogen loss. There is no doubt that a general improvement in the current state-of-the-art of vacuum annealing as practiced by the industry will have to be advanced in order to ensure that interstitial composition does not change during the required annealing treatment. This advancement will necessarily include the development of large bakeable ultra high vacuum furnaces capable of operation at up to approximately 4000°F.

### C. WELDABILITY

The effect of post weld annealing on the ductile-brittle transition temperature was determined on 0.04-inch sheet of ASTAR-811 and ASTAR-811CN which had been annealed for 1 hour at 1650°C and then TIG welded. Bead-on-plate type welds with 100% penetration were tested in bending over a 1t bend radius with the weld bead transverse to the bend axis. After welding specimens were annealed for 1 hour at 980, 1200, and 1425°C (1800, 2200, and 2600°F). The data obtained are recorded in Table 3. The ductile-brittle transition temperature of the solid solution alloy ASTAR-811 was less than -320°F as-TIG welded and did not change as a result of post-weld annealing. However, the transition temperature of the as-TIG welded ASTAR-811CN increased significantly after post-weld annealing with the higher post weld annealing temperature resulting in the greatest change. The increase in the ductile-brittle transition temperature for ASTAR-811CN summarized below is illustrated in Figure 5.

| DBTT<br>(°F) | 1 Hour<br>Post Weld Annealing<br>Temperature (°F) |
|--------------|---|
| -225         | As-Welded   |
| -200         | 1800  |
| -100         | 2200  |
| < 0          | 2600  |

**TABLE 3 - Ductile-Brittle Transition Temperature of Post (TIG) Weld Annealed NASV-23<sup>(a)</sup>**  
(Ta-7W-1Re-1Hf-0.012C-0.012N)

| Post Weld Anneal          | Test Temperature (°F) (°C) | No Load Bend Angle (Degrees) | Remarks  | DBTT |      |
|---------------------------|----------------------------|------------------------------|--|------|------|
|                           |                            |                              |  | (°F) | (°C) |
| As-TIG Welded             | -250 -157                  | 90                           | Failure Bend   | -225 | -143 |
|                           | -225 -143                  | 91                           |  |      |      |
| 1 Hr. at 980°C<br>1800°F  | -100 -73                   | 92                           | Bend Bend  | -200 | -129 |
|                           | -200 -129                  | 92                           |  |      |      |
|                           | -225 -143                  | 77                           | Brittle failure in weld<br>Brittle failure in weld and HAZ<br>Brittle failure in weld and HAZ  |      |      |
|                           | -250 -157                  | 44                           |  |      |      |
|                           | -320 -196                  | 30                           |  |      |      |
|                           |                            |                              |  |      |      |
| 1 Hr. at 1200°C<br>2200°F | -100 -73                   | 91                           | Bend   | -100 | -73  |
|                           | -125 -87                   | 77                           |  |      |      |
|                           | -150 -101                  | 26                           | Brittle failure in weld<br>Brittle failure in weld and HAZ   |      |      |
|                           | -200 -129                  | 37                           |  |      |      |
| 1 Hr. at 1425°C<br>2600°F | 75 23                      | 92                           | Bend   |      |      |
|                           | 50 10                      | 90                           |  |      |      |
|                           | 25 -4                      | 90                           | Very slight ductile failure in weld<br>Very slight ductile failure in weld<br>Very slight ductile failure in weld<br>Brittle failure in weld and HAZ |      |      |
|                           | 0 -18                      | 90                           |  |      |      |
|                           | -100 -73                   | 52                           |  |      |      |

(a) Specimens were all annealed for 1 hour at 1650°C (3000°F) prior to welding.

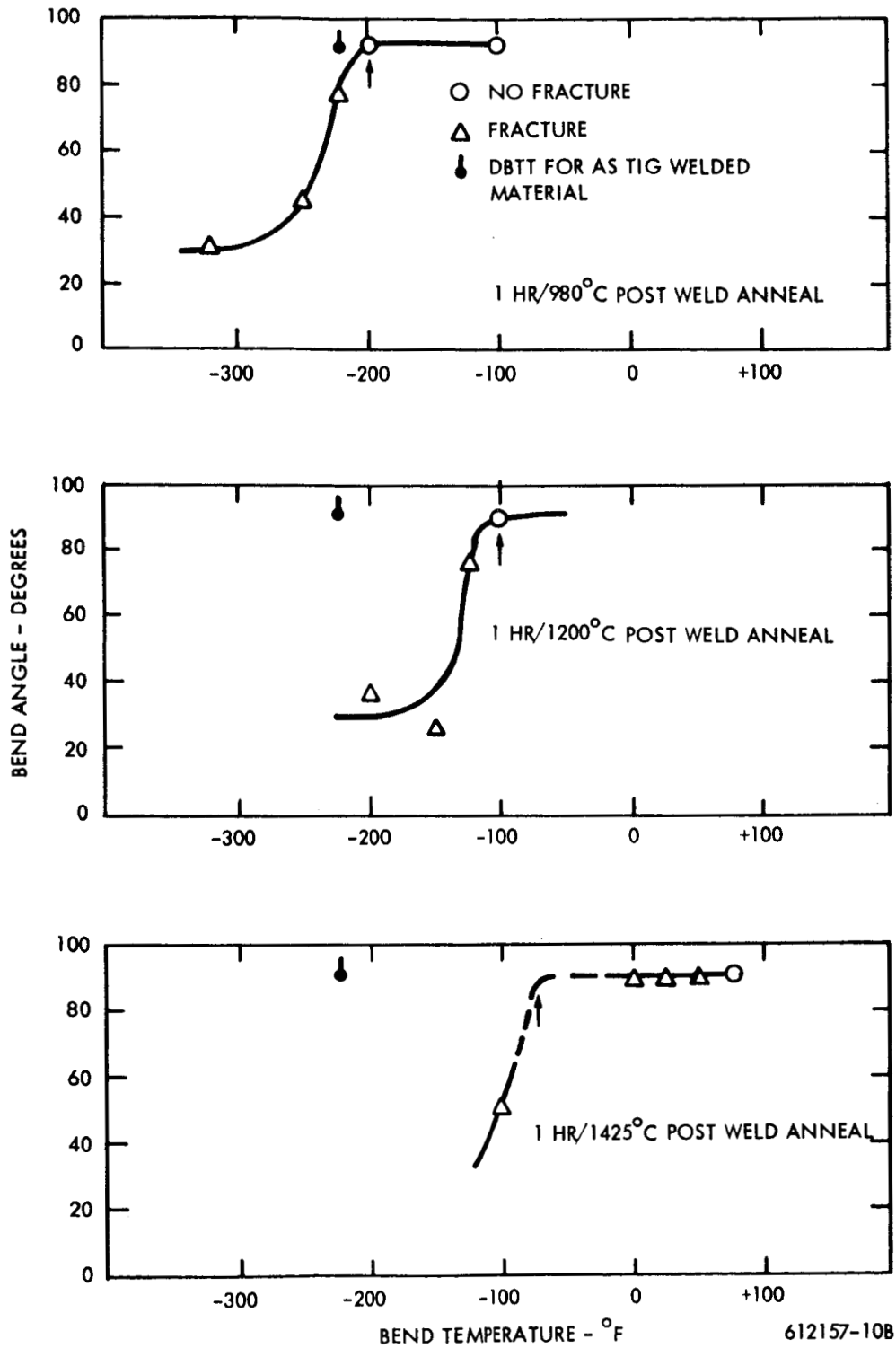


FIGURE 5 - Ductile-Brittle Transition Temperature Test Results for Post (TIG) Weld Annealed ASTAR-811CN (Ta-7W-1Re-1Hf-0.012C-0.012N)

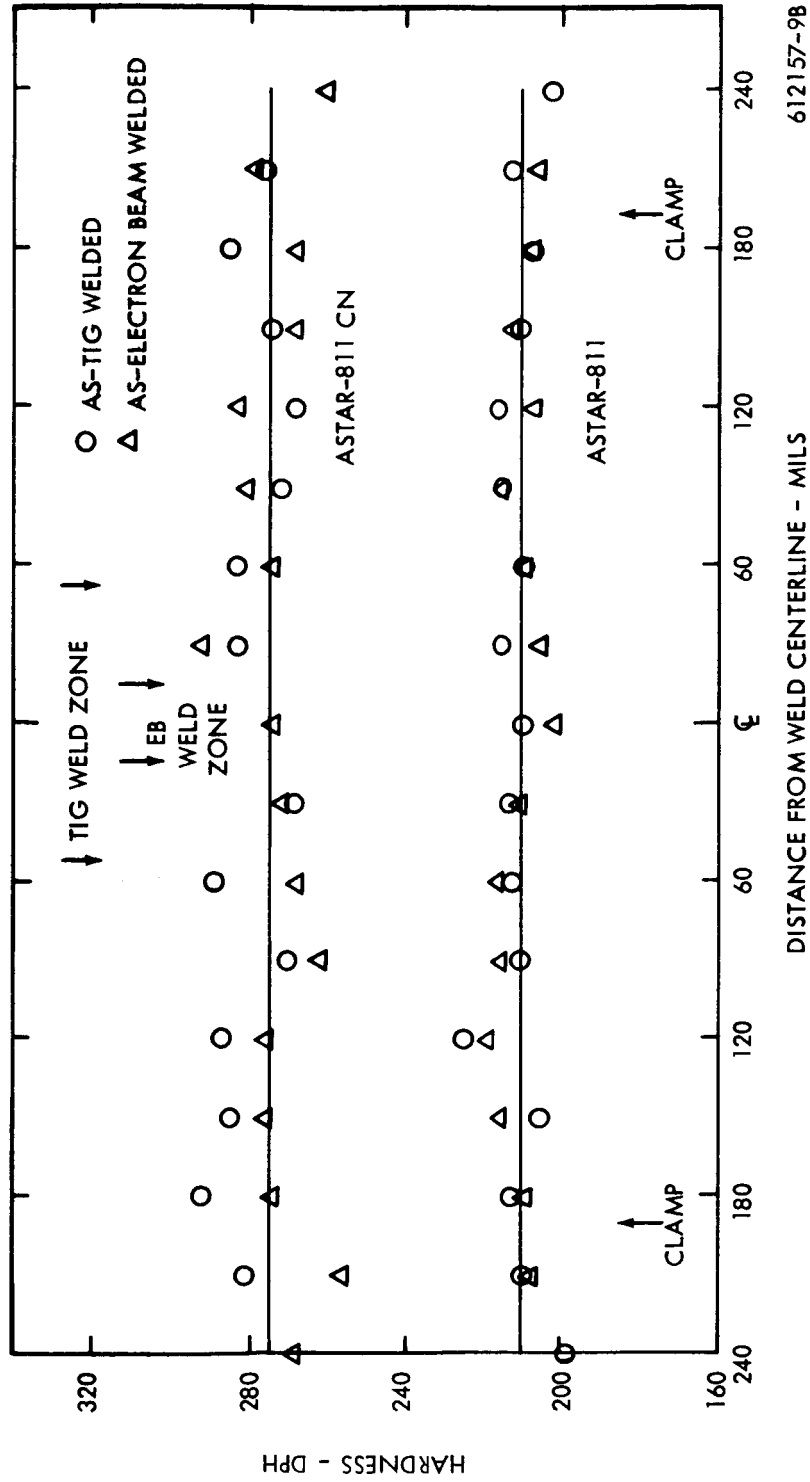
Failure occurred primarily within the weld and heat affected zones and appeared to be intergranular in nature.

Hardness traverses were made on transverse sections of as-electron beam and as-TIG welded sheet and post-weld annealed specimens of both alloys. The hardness traverses for as-electron beam and as-TIG welded ASTAR-811 and ASTAR-811CN sheet are shown in Figure 6. Little hardness variation was observed in either alloy across the base metal, weld, and heat affected zone. This same behavior was exhibited by the specimens which were post-weld annealed, although there was a decrease in hardness level of from 275 to 255 DPH for the ASTAR-811CN while that of the ASTAR-811 remained essentially unchanged.

The microstructures of the as-TIG welded ASTAR-811 and ASTAR-811CN were essentially single phase in the base metal, fusion, and heat affected zones. The few isolated precipitates observed are assumed to be primarily  $\text{HfO}_2$  in the ASTAR-811 and  $\text{Ta}_2\text{C}$  in the ASTAR-811CN. The photomicrographs in Figure 7 are typical of microstructures which were observed for ASTAR-811 and ASTAR-811CN in the as-welded condition.

The microstructure of the as-TIG welded ASTAR-811 remained essentially unchanged after the post weld annealing treatment. An exception however was that a sub-boundary network formed in the heat affected zone and some precipitation occurred near the weld/heat affected zone interface after post weld annealing for 1 hour at  $2200^\circ\text{F}$  (see Figure 8). Thus the post weld annealing treatments did not alter the ductile-brittle transition temperature of ASTAR-811 which is consistent with the observed absence of hardness and microstructural changes.

Post weld annealing ASTAR-811CN however did produce significant changes in the as-TIG welded single phase microstructure. The resulting microstructures produced by the 1 hour post weld anneals at 1800, 2200, and  $2600^\circ\text{F}$  are shown in Figure 9. Extensive precipitation occurred throughout the base metal, fusion, and heat affected zones during each of the post

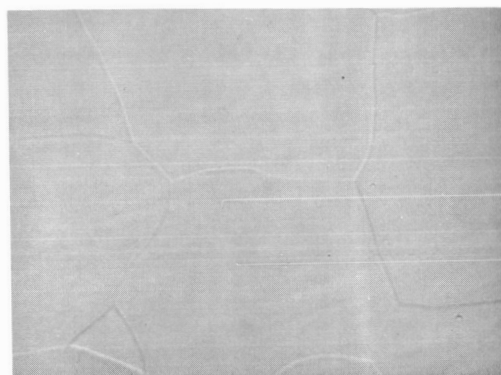


612157-9B

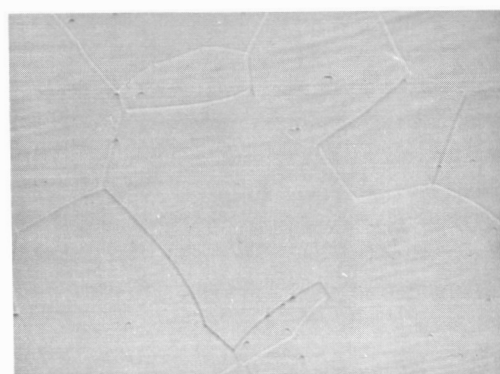
FIGURE 6 - Results of Hardness Traverses Across As-Welded Specimens of ASTAR-811 (Ta-8W-1Re-1Hf) and ASTAR-811CN (Ta-7W-1Re-1Hf-0.012C-0.012N)



(a) Weld Zone



(b) Heat Affected Zone



(c) Base Metal

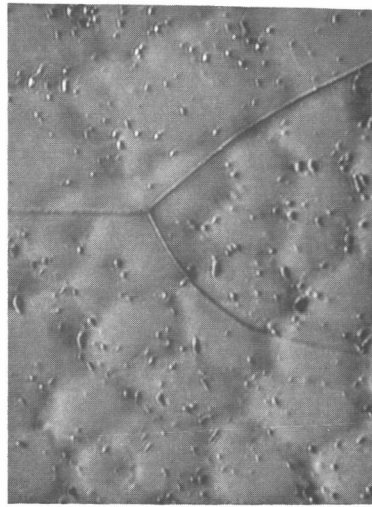
FIGURE 7 - Representative Microstructures of TIG Welded  
ASTAR-811 (Ta-8W-1Re-1Hf) 500X





1500X

FIGURE 8 - Microstructure of Weld Zone/Heat Affected Zone Interface in TIG Welded ASTAR-811 (Ta-8W-1Re-1Hf) Specimen After 1 Hr. Post Weld Anneal at 1200°C (2200°F)



Weld Zone

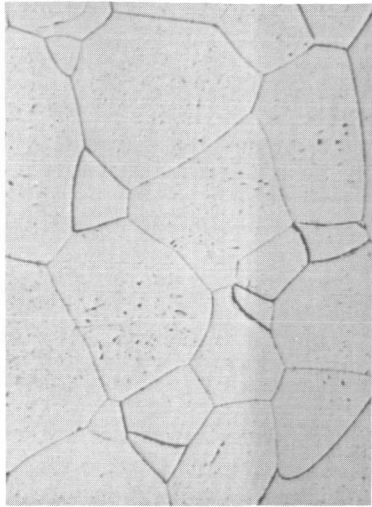
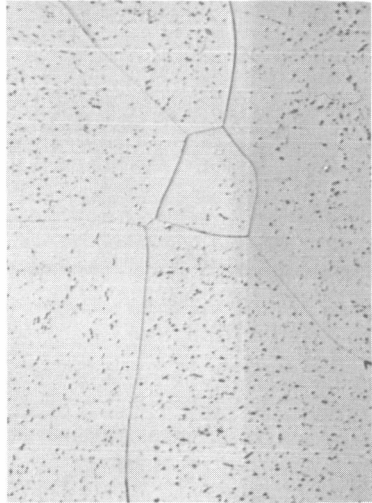
1500X

HAZ

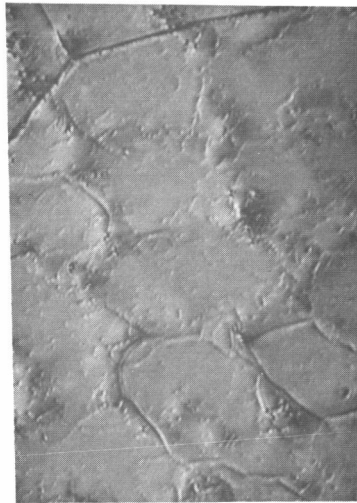
500X

Base Metal

500X



Post Weld Annealed for 1 Hour at 980°C (1800°F)



Weld Zone

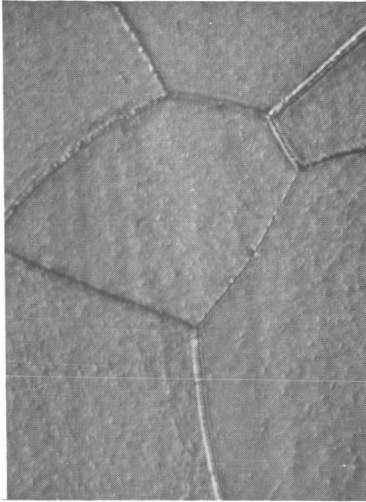
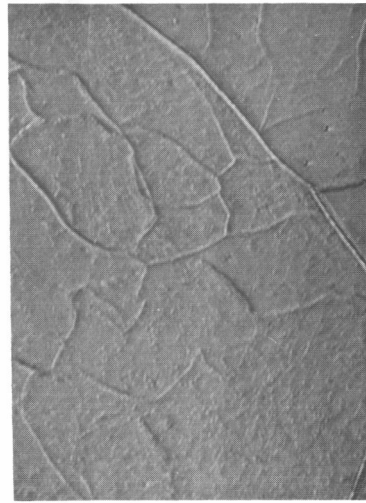
1500X

HAZ

1500X

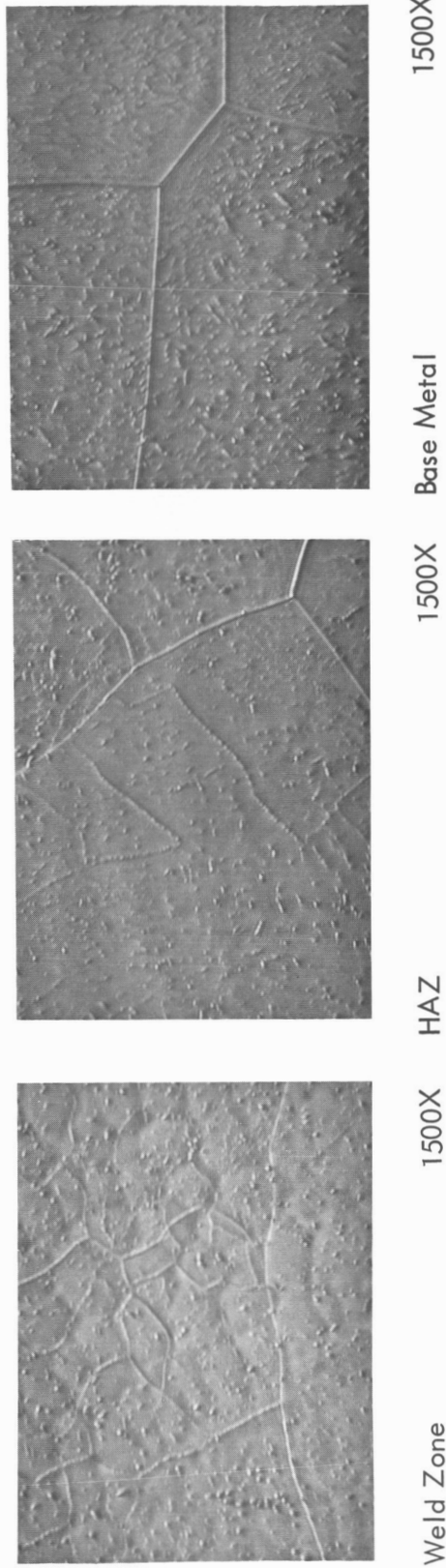
Base Metal

1500X



Post Weld Annealed for 1 Hour at 1200°C (2200°F)

FIGURE 9 - Microstructures of TIG Welded ASTAR-811CN (Ta-7W-1Re-1Hf-0.012C-0.012N) Specimens After 1 Hr. Post Weld Anneals at Various Temperatures



Post Weld Annealed for 1 Hour at 1425°C (2600°F)

FIGURE 9 (continued) – Microstructures of TIG Welded ASTAR-811CN (Ta-7W-1Re-1Hf-0.012C-0.012N) Specimens After 1 Hr. Post Weld Anneals at Various Temperatures

weld annealing treatments. The formation of this precipitate, which is most likely  $Ta_2C$ , no doubt accounts for the observed hardness decrease.

The distribution of the precipitate however did appear to be affected by the annealing temperature. At  $1800^{\circ}F$ , the precipitation occurred primarily throughout the matrix while at  $2200^{\circ}F$  and  $2600^{\circ}F$ , precipitates were formed at primary grain boundaries and cell and sub-boundaries in the fusion and heat affected zones. The cell and sub-boundary precipitates were larger after annealing at  $2600^{\circ}F$ . This change in precipitate distribution can thus be used to qualitatively explain the increase in ductile-brittle transition temperature with increasing post weld annealing temperature, particularly as the annealing temperature was increased from 1800 to  $2200^{\circ}F$ .

#### D. MECHANICAL PROPERTIES

1. Tensile Properties of TIG Welds — Bead-on-plate tungsten inert gas (TIG) welded specimens of ASTAR-811 and ASTAR-811CN were tested over the temperature range of  $-320$  to  $2600^{\circ}F$  ( $-195$  to  $1425^{\circ}C$ ) to evaluate the effects of welding on tensile properties. The welds, both longitudinal and transverse, were made on 0.04-inch thick sheet which had been annealed for 1 hour at  $1650^{\circ}C$  ( $3000^{\circ}F$ ) prior to welding. Tensile data are recorded in Table 4A along with the previously obtained data for ASTAR-811C. The tensile data for both ASTAR-811 and ASTAR-811CN appear to be anomalous in that the ductility values at room temperature were lower than those obtained at  $-195^{\circ}C$  ( $-320^{\circ}F$ ).

An additional set of room temperature tungsten inert gas (TIG) welded tensile specimens of each alloy were made and retested because of these anomalous results. Sections of 0.33-inch plate, processed from the side forgings, were annealed for 1 hour at  $1700^{\circ}C$  ( $3090^{\circ}F$ ) and rolled to 0.05-inch sheet, from which specimen blanks were obtained. These blanks were then annealed for 1 hour at  $1650^{\circ}C$  ( $3000^{\circ}F$ ) and the required transverse and longitudinal bead-on-plate TIG welds were made. Specimens, 0.04-inch thick, were machined from the welded blanks, x-rayed to ensure that no weld defects were present, and tested at room

TABLE 4A - Tensile Properties of TIG Welded ASTAR-811, ASTAR-811C,  
and ASTAR-811CN

| Composition and Heat No.   | Test Temp. (°F) | Weld Direction | 0.2% Yield Strength (ksi) | Ultimate Tensile Strength (ksi) | % Elongation |       |
|--|-----------------|----------------|---------------------------|---------------------------------|--------------|-------|
|  |                 |                |                           |                                 | Uniform      | Total |
| ASTAR-811<br>(Ta-8W-1Re-1Hf)<br>Heat NASV-22                     | -320            | Longitudinal   | 133.7                     | 157.0                           | 16.3         | 18.6  |
|  | -320            | Transverse     | 137.3                     | 160.6                           | 16.0         | 19.7  |
|  | RT              | Longitudinal   | 77.3                      | ---                             | 8.15         | 8.3   |
|  | RT              | Transverse     | 80.5                      | ---                             | 8.3          | 8.6   |
|  | 1800            | Longitudinal   | 36.2                      | 57.6                            | ---          | 18.1  |
|  | 2000            | Transverse     | 30.7                      | 47.2                            | ---          | 10.7  |
|  | 2400            | Longitudinal   | 27.8                      | 32.2                            | ---          | 6.6   |
|  | 2600            | Transverse     | 24.3                      | 28.5                            | ---          | 4.9   |
| ASTAR-811C<br>(Ta-8W-1Re-0.7Hf-<br>0.025C)<br>Heat NASV-20       | -320            | Longitudinal   | 157.3                     | 184.6                           | 16.7         | 24.2  |
|  | -320            | Transverse     | 159.0                     | 176.2                           | 10.9         | 14.2  |
|  | RT              | Longitudinal   | 109.8                     | 115.3                           | 15.0         | 28.5  |
|  | RT              | Transverse     | 89.3                      | 107.2                           | 10.6         | 18.7  |
|  | 1800            | Longitudinal   | 44.0                      | 67.1                            | ---          | 18.7  |
|  | 2400            | Longitudinal   | 35.3                      | 41.1                            | ---          | 29.0  |
|  | 2600            | Longitudinal   | 32.5                      | 36.0                            | ---          | 26.7  |
| ASTAR-811CN<br>(Ta-7W-1Re-1Hf-<br>0.012C-0.012N)<br>Heat NASV-23 | -320            | Longitudinal   | 166.4                     | ---                             | 5.25         | 5.4   |
|  | -320            | Longitudinal   | 163.0                     | 194.5                           | 17.4         | 22.5  |
|  | RT              | Transverse     | 106.3                     | 113.5                           | 9.7          | 11.3  |
|  | RT              | Transverse     | 110.8                     | 116.3                           | 9.6          | 15.4  |
|  | 1800            | Longitudinal   | 45.3                      | 70.6                            | ---          | 20.6  |
|  | 2000            | Transverse     | 40.0                      | 65.0                            | ---          | 16.4  |
|  | 2400            | Longitudinal   | 37.2                      | 45.4                            | ---          | 19.7  |
|  | 2600            | Transverse     | 31.0                      | 35.9                            | ---          | 21.5  |

**TABLE 4B - Tensile Properties of TIG Welded ASTAR-811 and ASTAR-811CN**

| Composition and Heat No.                                     | Test Temperature (°F) | Weld Direction | 0.2% Yield Strength (ksi) | Ultimate Tensile Strength (ksi) | % Elongation |       |
|--|-----------------------|----------------|---------------------------|---------------------------------|--------------|-------|
|  |                       |                |                           |                                 | Uniform      | Total |
| ASTAR-811<br>(Ta-8W-1Re-1Hf)<br>Heat NASV-22                 | -320                  | Longitudinal   | 134.6                     | 152.3                           | 17.50        | 22.15 |
|  | -320                  | Transverse     | 137.0                     | 148.0                           | 11.25        | 14.35 |
|  | RT                    | Longitudinal   | 77.6                      | 92.3                            | 14.60        | 19.15 |
|  | RT                    | Transverse     | 79.2                      | 90.9                            | 9.20         | 11.95 |
| ASTAR-811CN<br>(Ta-7W-1Re-1Hf-0.012C-0.012N)<br>Heat NASV-23 | -320                  | Longitudinal*  | 162.0                     | 188.0                           | 4.85         | 5.50  |
|  | -320                  | Transverse*    | 158.4                     | 189.8                           | 3.70         | 5.90  |
|  | RT                    | Longitudinal   | 109.0                     | 116.0                           | 13.15        | 22.70 |
|  | RT                    | Transverse     | 110.0                     | 114.0                           | 3.65         | 5.95  |

\*The stress-strain curves indicated that twinning may have occurred.

temperature and at  $-320^{\circ}\text{F}$ . The results are recorded in Table 4B. Where significant differences were noted, they are assumed to represent defective weldments in the original specimens. The test results for the ASTAR-811CN weldments indicate that the fracture mode is changing from ductile to brittle at  $-320^{\circ}\text{F}$ .

2. Creep Properties — Creep properties for 0.04-inch thick ASTAR-811 and ASTAR-811CN sheet were obtained at  $2200\text{--}2600^{\circ}\text{F}$  at stress levels of  $8,000\text{--}19,000$  psi. The data are recorded in Table 5. These data normalized using the Larson-Miller parameter are plotted in Figure 10 along with data for T-111 and ASTAR-811C. The creep strength of the solid solution composition ASTAR-811 is slightly better than T-111 but significantly inferior to both ASTAR-811C and ASTAR-811CN. The effects of the individual additions on creep strength at  $2400^{\circ}\text{F}$  and  $15,000$  psi are summarized below.

| Composition<br>w/o                           | Time to 1% Strain at $2400^{\circ}\text{F}$<br>and $15,000$ psi |
|--|---|
| Ta-8W-2Hf (T-111)                            | 20  |
| Ta-8W-1Re-1Hf (ASTAR-811)                    | 54  |
| Ta-8W-1Re-1Hf-0.025C (ASTAR-811C)            | 260   |
| Ta-7W-1Re-1Hf-0.012C-0.012N<br>(ASTAR-811CN) | 157   |

Although there is an apparent increase in creep resistance when rhenium is added to the tantalum matrix the increase may be due to the reduction of hafnium content, which has already been shown to exert a pronounced affect on creep strength.<sup>(1)</sup> There is however no doubt concerning the effect of the carbon and/or nitrogen additions on creep strength. Additional tests are underway to establish the stress and temperature dependence for each composition.

#### E. PHASE IDENTIFICATION

Information as to the identity of the precipitating phase(s) in the tantalum alloy matrix and their stability as a function of temperature and time is of vital importance.

TABLE 5 - Creep Properties of ASTAR-811 and ASTAR-811CN<sup>(a)</sup>

| Composition  | Test Temperature<br>(°F) | Stress<br>(psi) | Test Duration<br>(hrs.) | Total Elongation<br>(%) | Time to 1% Strain<br>(hrs.) | Vickers Hardness<br>DPH |           |
|--|--------------------------|-----------------|-------------------------|-------------------------|-----------------------------|-------------------------|-----------|
|  |                          |                 |                         |                         |                             | Pre-Test                | Post Test |
| ASTAR-811<br>(Ta-8W-1Re-1Hf)<br>(Heat NASV-22)                 | 2200                     | 19,000          | 826                     | 6.4                     | 185                         | 213                     | 212       |
|  | 2200                     | 15,000          | 1670                    | 0.66                    | ---                         | 213                     | 209       |
|  | 2400                     | 15,000          | 165                     | 4.6                     | 54                          |                         |           |
|  | 2400                     | 12,766          | 377                     | 1.3                     | 317                         | 209                     | 213       |
| ASTAR-811CN<br>(Ta-7W-1Re-1Hf-0.012C-0.012N)<br>(Heat NASV-23) | 2200                     | 19,000          | 835                     | 2.9                     | 607                         | 294                     | 241       |
|  | 2400                     | 15,000          | 426                     | 7.3                     | 157                         | 287                     | 228       |
|  | 2400                     | 12,500          | 530                     | 1.43                    | 403                         | 296                     | 228       |
|  | 2600                     | 8,000           | 382                     | 5.4                     | 172                         | 290                     | 245       |

(a) Specimens annealed at 1650°C for 1 hr. at  $1 \times 10^{-5}$  torr then tested at  $<1 \times 10^{-8}$  torr.



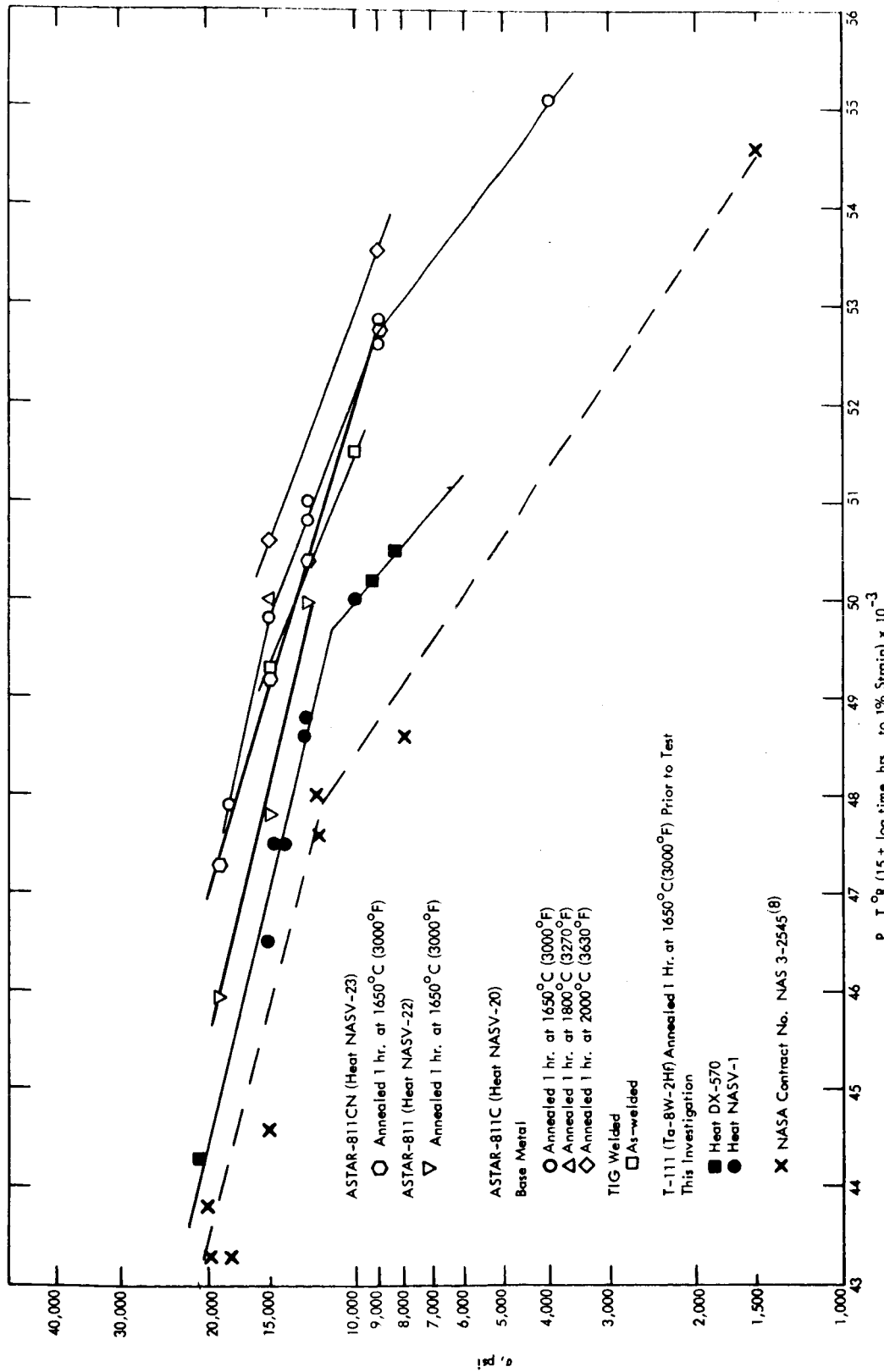


FIGURE 10 - Creep Properties of ASTAR Tantalum Alloys

Understanding of these phase relationships will aid in identifying the mechanism(s) contributing to the low and elevated temperature strength thus allowing more precise control over the final mechanical properties.

Prior work on the Ta-8W-1Re-1Hf-0.025C (ASTAR-811C) composition has shown that the dimetal carbide ( $Ta_2C$ ) is the only precipitating phase. It was also shown that the morphology of the  $Ta_2C$  precipitate could be significantly altered by thermal treatment. <sup>(4)</sup>

During this period, phase identification work has been carried out on the Ta-7W-1Re-1Hf-0.012C-0.012N composition (ASTAR-811CN). This alloy is essentially identical to ASTAR-811C except one half of the carbon has been replaced with an equivalent amount of nitrogen.

The dispersed phases present in the ASTAR-811CN at the various stages of processing from the as-cast ingot to 0.04 inch sheet were chemically extracted and analyzed by x-ray diffraction. The results which are recorded in Table 6 indicate only the presence of the HCP dimetal carbide  $Ta_2C$  ( $a_o = 3.10 - 3.11 \text{ \AA}$ ,  $c_o = 4.94 \text{ \AA}$ ,  $c/a = 1.59$ ). There is however very minor amounts of monoclinic  $HfO_2$  present which no doubt results from the residual oxygen. The amount of  $Ta_2C$  which occurred after annealing sheet at  $3000^\circ F$  and above is generally quite small since the carbon solvus for ASTAR-811CN is exceeded at or slightly above this temperature. No evidence of a nitride phase was detected and is consistent with previous work on tantalum alloy compositions containing 100-150 ppm nitrogen. <sup>(9)</sup>

Subsequent aging at lower temperatures was carried out over the temperature range of  $2000-2600^\circ F$  for times of 1 and 16 hours on ASTAR-811CN 0.04 inch sheet which had been solution annealed at  $3000^\circ F$  for 1 hour. Longer time aging treatments (up to 1000 hours) over this same temperature range are in progress and will be completed during the next report period. X-ray diffraction results on the residues chemically extracted from these specimens are listed in Table 7. Only  $Ta_2C$  was observed after aging for 1 and 16 hours up to  $2400^\circ F$

**TABLE 6 - X-ray Diffraction Analyses of Various ASTAR-811CN  
(Ta-7W-1Re-1Hf-0.012C-0.012N) Bulk Extracted Residues**

| Specimen  | Phases   | Comments |
|---|--|----------|
| As-cast   | HCP Ta <sub>2</sub> C                                | 1        |
| As-upset forged<br>at 1400°C (2550°F)           | HCP Ta <sub>2</sub> C<br>Mono HfO <sub>2</sub> (VW)  | 1        |
| Forged + annealed<br>(1 hr./1650°C (3000°F))    | HCP Ta <sub>2</sub> C<br>Mono HfO <sub>2</sub> (VW)  | 1        |
| As-rolled 0.06" sheet                           | HCP Ta <sub>2</sub> C                                | 1        |
| 0.06" sheet annealed<br>(1 hr./1700°C (3090°F)) | HCP Ta <sub>2</sub> C                                | 1        |
| As-rolled 0.04" sheet                           | HCP Ta <sub>2</sub> C<br>Mono HfO <sub>2</sub> (VVW) | 1        |
| 0.04" sheet annealed<br>(1 hr./1650°C (3000°F)) | HCP Ta <sub>2</sub> C                                | 1        |

NOTE: Approximate lattice parameters of all the HCP Ta<sub>2</sub>C phases were:

$$a_o = 3.10 \text{ to } 3.11 \overset{\circ}{\text{A}} \quad c_o = 4.94 \overset{\circ}{\text{A}} \quad c/a = 1.59$$

VW - VeryWeak, VVW - Very Very Weak

(1) Diffraction lines partially resolved

**TABLE 7 - X-ray Diffraction Analyses of Phases Extracted from ASTAR-811CN (Ta-7W-1Re-1Hf-0.012C-0.012N) Specimens Annealed for 1 Hour at 1650°C and Aged for 1 and 16 Hours at 1090, 1200, 1315, and 1425°C.**

| Specimen  | Phases                      | Comments                 |
|---|-----------------------------|--------------------------|
| 0.04" sheet annealed<br>(1 hr./1650°C (3000°F)) | HCP Ta <sub>2</sub> C       | 1                        |
| +(1 hr./1090°C (2000°F))                        | HCP Ta <sub>2</sub> C       | 1                        |
| +(1 hr./1200°C (2200°F))                        | HCP Ta <sub>2</sub> C       |                          |
| +(1 hr./1315°C (2400°F))                        | HCP Ta <sub>2</sub> C       |                          |
|   | Mono HfO <sub>2</sub> (VVW) |                          |
| +(1 hr./1425°C (2600°F))                        | HCP Ta <sub>2</sub> C       | 1                        |
|   | Mono HfO <sub>2</sub> (VW)  |                          |
| +(16 hrs./1090°C (2000°F))                      | HCP Ta <sub>2</sub> C       |                          |
| +(16 hrs./1200°C (2200°F))                      | HCP Ta <sub>2</sub> C       |                          |
|   | Mono HfO <sub>2</sub> (VVW) |                          |
| +(16 hrs./1315°C (2400°F))                      | HCP Ta <sub>2</sub> C       | 1                        |
|   | Mono HfO <sub>2</sub> (VVW) |                          |
| +(16 hrs./1425°C (2600°F))                      | HCP Ta <sub>2</sub> C (S)   | 1                        |
|   | Mono HfO <sub>2</sub> (VW)  |                          |
|   | FCC Hf(CN) (M)              | $a_o = 4.56 \text{ \AA}$ |

NOTE: Approximate lattice parameters of all the HCP Ta<sub>2</sub>C phases were:

$$a_o = 3.10 \text{ to } 3.11 \text{ \AA} \quad c_o = 4.94 \text{ \AA} \quad c/a = 1.59$$

(1) Diffraction lines partially resolved

and after 1 hour at 2600°F. However, after 16 hours at 2600°F, a FCC phase, most likely Hf(CN), is beginning to form. Accompanying the formation of the Ta<sub>2</sub>C and Hf(CN) precipitate is a drop in the room temperature hardness (See Figure 11). The largest change in hardness occurred after the first hour which is indicative of the rapid precipitation kinetics of the carbide precipitation reaction. The room temperature hardness after aging for 16 hours at 2000, 2200, and 2400°F is similar. However there is a definite increase in the hardness level for specimens aged at 2600°F which may reflect the higher interstitial solubility or may be related to the nitride precipitation reaction. The appearance of the FCC phase was not unexpected since a similar composition tested early in this investigation exhibited the same behavior.<sup>(9)</sup>

### III. FUTURE WORK

During the next period the following will be accomplished.

1. Initiate creep testing of controlled grain size creep specimens.
2. Continue investigation on the effect of long time annealing treatments on the phase morphology and stability of the ASTAR-811C and ASTAR-811CN.
3. Complete 500 hour annealing treatment at 2200°F on TIG welded ASTAR-811CN (Heat NASV-23) and determine ductile brittle transition temperature.

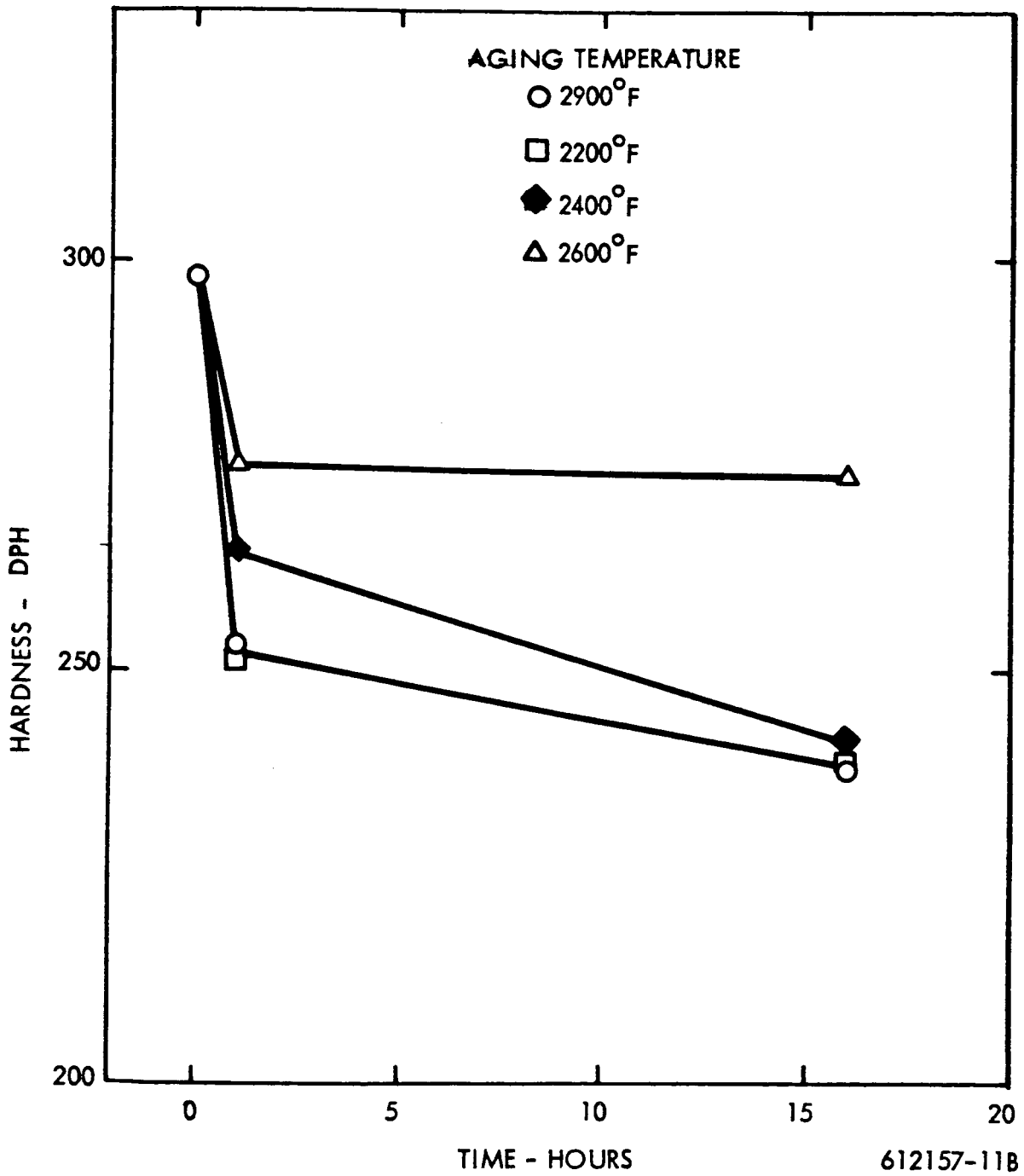


FIGURE 11 - Aging Behavior of ASTAR-811CN  
(Annealed 1 Hr. at 3000°F Prior to Aging)

#### IV. REFERENCES

1. R. W. Buckman, Jr. and R. T. Begley, "Development of Dispersion Strengthened Tantalum Base Alloy", Final Technical Report, Phase I, WANL-PR-(Q)-004.
2. R. W. Buckman, Jr. and R. C. Goodspeed, "Development of Dispersion Strengthened Tantalum Base Alloy", 11th Quarterly Progress Report, WANL-PR(Q)-012, NASA-CR-72094.
3. R. W. Buckman, Jr. and R. C. Goodspeed, "Development of Dispersion Strengthened Tantalum Base Alloy", 12th Quarterly Progress Report, WANL-PR(Q)-013, NASA-CR-
4. R. W. Buckman, Jr. and R. C. Goodspeed, "Development of Dispersion Strengthened Tantalum Base Alloy", 10th Quarterly Progress Report, WANL-PR-(Q)-011, NASA-CR-72093.
5. R. Resnick and L. J. Castleman, 1960 Trans. AIME, 218, 307.
6. R. W. Buckman, Jr., "Development of Dispersion Strengthened Tantalum Base Alloy", 5th Quarterly Progress Report, WANL-PR-(Q)-006, NASA-CR-4462.
7. R. W. Buckman, Jr. and R. T. Begley, "Development of Dispersion Strengthened Tantalum Base Alloy", 3rd Quarterly Progress Report, WANL-PR-(Q)-003, NASA-CR-54105.
8. J. Sawyer and E. A. Steigerwald, "Generation of Long Time Creep Data of Refractory Metal Alloys at Elevated Temperature", 12th Quarterly Report, NAS-CR-72044, NASA Contract 3-2545.
9. R. W. Buckman, Jr. and R. C. Goodspeed, "Development of Dispersion Strengthened Tantalum Base Alloy", 6th Quarterly Progress Report, WANL-PR-(Q)-007, NASA-CR-54658.

DISTRIBUTION LIST

TRW  
Caldwell Research Center  
23555 Euclid Avenue  
Cleveland, Ohio 44117  
Attn: Librarian  
Attn: G. J. Guarnieri

TRW  
New Devices Laboratories  
7209 Platt Avenue  
Cleveland, Ohio 44104  
Attn: Librarian

National Aeronautics & Space Adm.  
Washington, D. C. 20546  
Attn: Walter C. Scott  
Attn: James J. Lynch (RN)  
Attn: George C. Deutsch (RR)  
Attn: S. V. Manson

National Aeronautics & Space Adm.  
Scientific and Technical Inf. Facility  
Box 5700  
Bethesda, Maryland 21811

NASA-Ames Research Center  
Moffet Field, California 94035  
Attn: Librarian

NASA-Goddard Space Flight Center  
Greenbelt, Maryland 20771  
Attn: Librarian

NASA-Langley Research Center  
Hampton, Virginia 23365  
Attn: Librarian

NASA-Manned Spacecraft Center  
Houston, Texas 77001  
Attn: Librarian

NASA-Jet Propulsion Laboratory  
4800 Oak Grove Drive  
Pasadena, California 91103  
Attn: Librarian

NASA-Lewis Research Center  
21000 Brookpark Road  
Cleveland, Ohio 44135

Attn: Librarian  
Attn: Dr. Bernard Lubarsky  
Attn: Mr. R. L. Cummings  
Attn: Mr. G. M. Ault  
Attn: Mr. J. Joyce  
Attn: Mr. P. E. Moorhead  
Attn: Mr. N. T. Musial  
Attn: Mr. T. Strom  
Attn: Mr. T. A. Moss  
Attn: Dr. Louis Rosenblum  
Attn: J. Creagh  
Attn: Mr. J. Dilley  
Attn: Mr. J. J. Fackler  
Attn: Mr. I. I. Pinkel  
Attn: Mr. G. Tulsiaik  
Attn: Mr. W. D. Klopp  
Attn: Mr. C. Hoffman  
Attn: NASA-Lewis Lab. Report Central  
Section

NASA- Western Operations Office  
150 Pico Boulevard  
Santa Monica, California 90406  
Attn: Mr. John Keeler

National Bureau of Standards  
Washington 25, D. C.  
Attn: Librarian

NASA-George C. Marshall Space Flight Center  
Huntsville, Alabama 35812  
Attn: Librarian  
Attn: Wm. A. Wilson



Aeronautical Systems Division  
Wright-Patterson Air Force Base, Ohio  
Attn: Charles Armbruster  
Attn: T. Cooper  
Attn: Librarian  
Attn: John L. Morris  
Attn: H. J. Middendorp  
Attn: G. Thompson  
Attn: G. Sherman

Army Ordnance Frankford Arsenal  
Bridesburg Station  
Philadelphia 37, Pennsylvania  
Attn: Librarian

Bureau of Ships  
Dept. of the Navy  
Washington 25, D. C.  
Attn: Librarian

Bureau of Weapons  
Research and Engineering  
Material Division  
Washington 25, D. C.  
Attn: Librarian

U. S. Atomic Energy Commission  
Technical Reports Library  
Washington 25, D. C.  
Attn: J. M. O'Leary

U. S. Atomic Energy Commission  
Germantown, Maryland  
Attn: Col. E. L. Douthett  
Attn: H. Rothen  
Attn: Major Gordon Dicker

U. S. Atomic Energy Commission  
Technical Information Service Extension  
P. O. Box 62  
Oak Ridge, Tennessee

U. S. Atomic Energy Commission  
Washington 25, D. C.  
Attn: M. J. Whitman

Argonne National Laboratory  
9700 South Cross Avenue  
Argonne, Illinois  
Attn: Librarian

Brookhaven National Laboratory  
Upton, Long Island, New York  
Attn: Librarian

Oak Ridge National Laboratory  
Oak Ridge, Tennessee  
Attn: W. O. Harms  
Attn: Dr. A. J. Miller  
Attn: Librarian  
Attn: N. T. Bray

Office of Naval Research  
Power Division  
Washington 25, D. C.  
Attn: Librarian

U. S. Naval Research Laboratory  
Washington 25, D. C.  
Attn: Librarian

Advanced Technology Laboratories  
Division of American Standard  
369 Whisman Road  
Mountain View, California  
Attn: Librarian

Aerojet General Corporation  
P. O. Box 296  
Azusa, California  
Attn: Librarian

Aerojet General Nucleonics  
P. O. Box 77  
San Ramon, California  
Attn: Librarian

AiResearch Manufacturing Company  
Sky Harbor Airport  
402 South 36th Street  
Phoenix, Arizona  
Attn: Librarian  
Attn: E. A. Kovacevich

AiResearch Manufacturing Company  
9851-9951 Sepulveda Boulevard  
Los Angeles 45, California  
Attn: Librarian

I. I. T. Research Institute  
10 W. 35th Street  
Chicago, Illinois 60616

Atomics International  
8900 DeSoto Avenue  
Canoga Park, California 91304  
Attn: W. Botts

Avco  
Research & Advanced Development Dept.  
201 Lowell Street  
Wilmington, Massachusetts  
Attn: Librarian

Babcock and Wilcox Company  
Research Center  
Alliance, Ohio  
Attn: Librarian

Battelle Memorial Institute  
505 King Avenue  
Columbus, Ohio  
Attn: C. M. Allen  
Attn: Librarian  
Attn: Defense Metals Inf. Center

The Bendix Corporation  
Research Laboratories Division  
Southfield, Detroit 1, Michigan  
Attn: Librarian

Bell Aerosystems Co.  
P. O. Box 1  
Buffalo 5, New York  
Attn: E. J. King

The Boeing Company  
Seattle, Washington  
Attn: Librarian

Brush Beryllium Company  
17876 St. Clair Avenue  
Cleveland, Ohio 44110  
Attn: Librarian

Carborundum Company  
Niagara Falls, New York  
Attn: Librarian

Chance Vought Aircraft Inc.  
P. O. Box 5907  
Dallas 22, Texas  
Attn: Librarian

Clevite Corporation  
Mechanical Research Division  
540 East 105th Street  
Cleveland 8, Ohio  
Attn: Mr. N. C. Beerli

Climax Molybdenum Company of Michigan  
1600 Huron Parkway  
Ann Arbor, Michigan  
Attn: Librarian

Convair Astronautics  
50001 Kerry Villa Road  
San Diego 11, California  
Attn: Librarian

E. I. duPont deNemours and Co., Inc.  
Wilmington 98, Delaware  
Attn: Librarian

Electro-Optical Systems, Inc.  
Advanced Power Systems Division  
Pasadena, California  
Attn: Librarian

Fansteel Metallurgical, Corp.  
North Chicago, Illinois  
Attn: Librarian



**Astronuclear  
Laboratory**

Ford Motor Company  
Aeronutronics  
Newport Beach, California  
Attn: Librarian

General Dynamics/General Atomic  
P. O. Box 608  
San Diego, California 92112  
Attn: Librarian

General Electric Company  
Atomic Power Equipment Div.  
P. O. Box 1131  
San Jose, California

General Electric Company  
Flight Propulsion Laboratory Dept.  
Cincinnati 15, Ohio  
Attn: Librarian  
Attn: Dr. J.W. Semmel

General Electric Company  
Missile and Space Vehicle Dept.  
3198 Chestnut Street  
Philadelphia 4, Pennsylvania  
Attn: Librarian

General Electric Company  
Vallecitos  
Vallecitos Atomic Lab.  
Pleasanton, California  
Attn: Librarian

Herring Corp.  
7356 Greenback Drive  
Hollywood, California 91605  
Attn: Don Adams

General Dynamics/Fort Worth  
P. O. Box 748  
Fort Worth, Texas  
Attn: Librarian

General Motors Corporation  
Allison Division  
Indianapolis 6, Indiana  
Attn: Librarian

Hamilton Standard  
Div. of United Aircraft Corp.  
Windsor Locks, Connecticut  
Attn: Librarian

Hughes Aircraft Company  
Engineering Division  
Culver City, California  
Attn: Librarian

Lockheed Missiles and Space Div.  
Lockheed Aircraft Corp.  
Sunnyvale, California  
Attn: Librarian

Marquardt Aircraft Co.  
P. O. Box 2013  
Van Nuys, California  
Attn: Librarian

The Martin Company  
Baltimore 3, Maryland  
Attn: Librarian

The Martin Company  
Nuclear Division  
P. O. Box 5042  
Baltimore 20, Maryland  
Attn: Librarian

Martin Marietta Corp.  
Metals Technology Laboratory  
Wheeling, Illinois

Massachusetts Institute of Technology  
Cambridge 39, Massachusetts  
Attn: Librarian

Materials Research and Development  
Manlabs Inc.  
21 Erie Street  
Cambridge 39, Massachusetts

Materials Research Corporation  
Orangeburg, New York  
Attn: Librarian

McDonnell Aircraft  
St. Louis, Missouri  
Attn: Librarian

MSA Research Corporation  
Callery, Pennsylvania  
Attn: Librarian

North American Aviation  
Los Angeles Division  
Los Angeles 9, California  
Attn: Librarian

National Research Corp.  
Metals Division  
45 Industrial Place  
Newton, Massachusetts 02164  
Attn: Dr. M. L. Torte  
Director of Metallurgical Research

Lawrence Radiation Laboratory  
Livermore, California  
Attn: Dr. James Hadley  
Head, Reactor Division

Pratt & Whitney Aircraft  
400 Main Street  
East Hartford 8, Connecticut  
Attn: Librarian

Republic Aviation Corporation  
Farmingdale, Long Island, New York  
Attn: Librarian

Solar  
2200 Pacific Highway  
San Diego 12, California

Southwest Research Institute  
8500 Culebra Road  
San Antonio 6, Texas  
Attn: Librarian

Rocketdyne  
Canoga Park, California  
Attn: Librarian

Superior Tube Co.  
Norristown, Pennsylvania  
Attn: Mr. A. Bound

Sylvania Electric Products, Inc.  
Chem. & Metallurgical  
Towanda, Pennsylvania  
Attn: Librarian

Temescal Metallurgical  
Berkeley, California  
Attn: Librarian

Union Carbide Stellite Corp.  
Kokomo, Indiana  
Attn: Librarian

Union Carbide Metals  
Niagara Falls, New York  
Attn: Librarian

Union Carbide Nuclear Company  
P. O. Box X  
Oak Ridge, Tennessee  
Attn: X-10 Laboratory Records Department

United Nuclear Corporation  
Research & Engineering Center  
Grassland Road  
Elmsford, New York 10523  
Attn: Librarian  
Attn: Mr. Albert Weinstein



**Astronuclear  
Laboratory**

Universal Cyclops Steel Corp.  
Refractomet Division  
Bridgeville, Pennsylvania  
Attn: C. P. Mueller

TRW Space Technology Laboratories  
One Space Park  
Redondo Beach, California  
Attn: Librarian

University of California  
Lawrence Radiation Lab.  
P. O. Box 808  
Livermore, California  
Attn: Librarian

University of Michigan  
Department of Chemical & Metallurgical Eng.  
Ann Arbor, Michigan  
Attn: Librarian

Vought Astronautics  
P. O. Box 5907  
Dallas 22, Texas  
Attn: Librarian

Wolverine Tube Division  
Calumet & Hecla, Inc.  
17200 Southfield Road  
Allen Park, Michigan  
Attn: R. C. Cash

Wyman-Gordon Co.  
North Grafton, Massachusetts  
Attn: Librarian

Wah Chang Corporation  
Albany, Oregon  
Attn: Librarian

Lawrence Radiation Laboratory  
P. O. Box 808  
Livermore, California 94551  
Attn: Richard R. Vandervoort